ORIGINAL ARTICLE

# Study of the influence of ascorbyl palmitate and amiodarone in the stability of unilamellar liposomes

Luciano Benedini[1], Silvia Antollini[2], Maria Laura Fanani[3], Santiago Palma[4], Paula Messina[1], and Pablo Schulz[1]

[1]Instituto de Química del Sur (INQUISUR – CONICET), Departamento de Química, [2]Instituto de Investigaciones bioquímicas de Bahía Blanca (INIBIBB – CONICET), Universidad Nacional del Sur, Bahía Blanca, Argentina, [3]Centro de Investigaciones en Química Biológica de Córdoba (CIQUIBIC – CONICET), Departamento de Química Biológica, and [4]Unidad de Investigación y Desarrollo en Tecnología Farmacéutica (UNITEFA – CONICET), Departamento de Farmacia, Facultad de Ciencias Químicas, Universidad Nacional de Córdoba, Ciudad Universitaria, Córdoba, Argentina

## Abstract

Amiodarone (AMI) is a low water-solubility drug, which is very useful in the treatment of severe cardiac disease. Its adverse effects are associated with toxicity in different tissues. Several antioxidants have been shown to reduce, and prevent AMI toxicity. The aim of this work was to develop and characterize Dimyristoylphosphatidylcholine (DMPC) liposomal carriers doped with ascorbyl palmitate ($Asc_{16}$) as antioxidant, in order to either minimize or avoid the adverse effects produced by AMI. The employment of liposomes would avoid the use of cosolvents in AMI formulations, and $Asc_{16}$ could minimize the adverse effects of AMI. To evaluate the partition and integration of AMI and $Asc_{16}$ in lipid membranes, penetration studies into DMPC monolayers were carried out. The disturbance of the liposomes membranes was studied by generalized polarization (GP). The stability of liposomes was evaluated experimentally and by means of the Derjaguin-Landau-Verwey-Overbeek (DLVO) theory. The size particle and zeta potential ($\zeta$) values of the liposomes were used for application in calculations for attractive and repulsive forces in DLVO theory. In experimental conditions all of these vesicles showed stability at time 0, but only DMPC + $Asc_{16}$ 10% + AMI 10% liposomes kept their size stable and $\zeta$ during 28 days. These results are encouraging and suggest that such systems could be suitable for AMI delivery formulations.

## Introduction

Amiodarone (2-butylbenzofuran-3-yl 4-(2-diethylaminoethoxy)-3,5-di-iodophenyl ketone) (AMI) (M.M: 645.3) is a cationic amphiphilic molecule at neutral and acidic pHs (pKa ~6.6 at 25 °C) (Boury et al., 2001) (Figure 1a: AMI molecule). It is a class III antiarrhythmic drug and is used in the control of ventricular and supraventricular arrhythmias, including those associated with Wolff-Parkinson-White (WPW) syndrome. AMI is usually administrated through intravenous infusion (Sweetman, 2009, p. 1211).

Adverse cardiovascular effects and others are common with AMI. Many of them are dose-related and reversible with reduction in doses (Sweetman, 2009, p. 1211). It was suggested in reference (Sweetman, 2009, p. 1212), that amiodarone-induced phospholipidosis (PLD) and this fact may explain some of these adverse effects. The PLD is a storage disorder characterized by the excessive accumulation of phospholipids in tissues (Anderson & Borlak, 2006). The mechanism of the PLD is not entirely clear. However,

it was suggested (Vereckei et al., 1993) that oxidative stress, a process that generates free radicals, is involved in the pathogenesis produced by AMI. Moreover, external factors, such as light, can exacerbate the AMI side-effects. Photosensitivity reactions, produced by light exposure in presence of the drug, are also common. This is a skin reaction produced by accumulation of AMI and light action that generates a reactive oxygen species and consequently develops the peroxidation of lipid chains in cell membranes and other intracellular structures (Stratton & Liebler, 1997). It has been reported in literature (Kachel et al., 1990) that photoprotective agents such as beta-carotene and vitamin E may reduce reactive oxygen species and thereby reduce the AMI phototoxicity. Kachel et al. (1990) reported that vitamin E reduces pulmonary cytotoxicity produced by AMI. It was also reported that vitamin E and a sylimarina, a type of flavonoid, decrease PLD induced by AMI (Agoston et al., 2003). Other authors (Ray et al., 2000), reported that proanthocyanidins from grape seeds are antioxidants potentially used in the treatment of PLD induced by AMI. The use of antioxidants is theoretically a form to either repair or minimize photosensitivity and other reactions produced by PLD.

Ascorbyl palmitate ($Asc_{16}$) (Figure 1b) is a good antioxidant in model cell systems (Lo Nostro, 1997). It is known that

Correspondence: Dr Luciano Benedini, Instituto de Química del Sur (INQUISUR – CONICET), Departamento de Química, Universidad Nacional del Sur, 8000 FTN Bahía Blanca, Argentina. Tel: +54 291 4595101. E-mail: lbenedini@uns.edu.ar
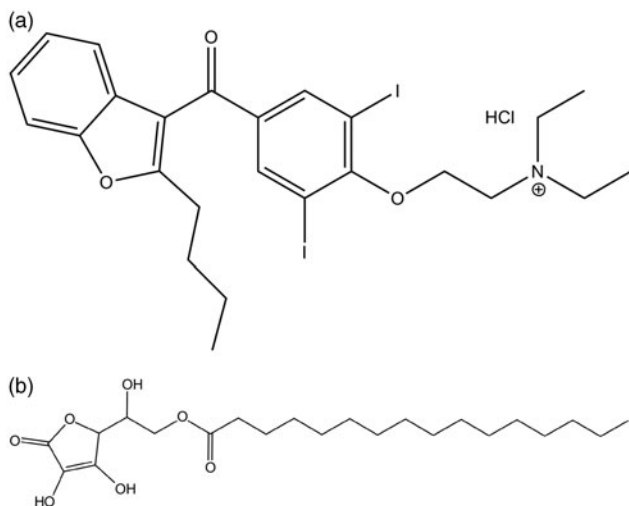
RIGHTSLINK

Figure 1. Chemical structure of (a) amiodarone, and (b) ascorbyl palmitate.

$Asc_{16}$ retains the same radical-scavenging properties of ascorbic acid and their antioxidant efficiency is comparable to that of other natural reducing agents, such as carotenes, polyphenols, and tocopherols (Sweetman, 2009, p. 1629). Their amphiphilic nature allows these vitamin C derivatives to form aggregates that provide an ideal environment for the solubilization of hydrophobic and sensitive drugs that might otherwise be easily degraded and oxidized when exposed to light, heat, dissolved oxygen, and other radical-producing species (Lo Nostro et al., 2003, Benedini et al., 2011b). The antioxidant characteristics of $Asc_{16}$ mean that it could be used to reduce or avoid AMI side-effects.

Due to the low aqueous solubility of amiodarone to develop an injectable formulation, surfactants and cosolvents addition are required. Then, marketed formulations are compounded with amiodarone hydrochloride (50 mg/ml), polysorbate 80 (Tween 80, 100 mg/ml) and benzyl alcohol (20 mg/ml) generally in 3 ml ampoules (Benedini et al., 2010). In addition, the excipients make amiodarone solubilization in aqueous solution possible, and can also contribute to the appearance of other kinds of side-effects such as negative inotropy and hypotension (Gough et al., 1982; Yasaka et al., 1979).

The AMI adverse effects and the use of cosolvents to solubilizate it, lead to unwavering search for drug carriers systems less harmful to humans. Systems that fulfill these principles are liposomes, given that these colloidal carriers are formed by phospholipids and other biocompatible components that do not produce adverse effects. Liposomes can be made entirely from natural substances and therefore are non-toxic, biodegradable and non-immunogenic (Lasic, 1998). A binary phospholipid-$Asc_{16}$ liposome system is proposed here as suitable to be used as a stable drug carrier where both components coexist with a reasonably favorable interaction. This behavior is supported by previous studies where $Asc_{16}$ show a great tendency to integrate into phospholipid monolayers adding stability to these supramolecular structures (Mottola et al., 2013). The aim of this work was to develop liposomes formed by phospholipids and $Asc_{16}$ with characteristics assessed by extrapolation from monolayer adsorption/penetration studies. AMI favorable incorporation to the binary phospholipid-$Asc_{16}$ membranes was evidenced in monolayer penetration studies. Both phospholipid-$Asc_{16}$ and phospholipid-$Asc_{16}$-AMI liposome systems have been studied by generalized polarization (GP). Liposome dispersions are not stable thermodynamically (Lasic, 1998), but measurements of stability were performed and, during 28 days, the liposomes containing DMPC + $Asc_{16}$ 10% + AMI 10% showed stability in either their size and z potential. This can be attributed to an increase of negative charge induced by $Asc_{16}$ and a structured effect induced by AMI to the ternary liposomes that keep them in a stable dispersion and decrease their aggregation. Furthermore, it is important to remark that this behavior is in accord with the predictions performing by DLVO theory. This theory explains the stability of lyophobic colloidal systems given that two independent types of forces govern the interaction between similar colloidal particles immersed in polar (especially aqueous) solutions: Attractive van der Waals forces and repulsive electrostatic forces (Derjaguin & Landau, 1941; Verwey & Overbeek, 1948). Here DLVO theory has been extended by introducing the hydrated radius of the ions adsorbed onto the liposome surfaces. Liposomes size, size distribution and zeta potentials ($\zeta$) data were applied in DLVO theory.

## Experimental section

### Materials

Ascorbyl palmitate ($Asc_{16}$) was purchased from Fluka (Italy) (MW: 414.53), Amiodarone (M.M: 645.3) was from Parafam (Argentine). Dimyristoylphosphatidylcholine (DMPC) was provided by Avanti Polar Lipids Inc. (Alabaster, AL) and Laurdan was from Molecular Probes (Eugene, OR). All the reagents were of analytical grade (99% pure) and used without further purification. Solvents were of the highest commercial purity available. The water was purified by using a Milli-Q (Millipore, Billerica, MA) system, giving a product with a resistivity of $\sim$18.5 M$\Omega$/cm.

### Methods

#### Adsorption of AMI to bare air/water interface

After the injection of the drug (75 μl of AMI solution) in ethanol to the aqueous subphase of a Teflon trough under continuous stirring (trough volume: 15 ml; final subphase concentration unless indicated was 15.5 μM of AMI), the changes in surface pressure and surface potential at constant area were registered as a function of time, while a Gibbs monolayer was established. A control with ethanol alone was used to check that surface pressure was not affected. Surface pressure was determined by a Pt plate using the Wilhelmy method, and the Volta surface potential ($\Delta V$) was monitored using an air-ionizing [241]Am surface electrode placed $\sim$5 mm above the interface and a Ag/AgCl/Cl⁻ (3M) reference electrode dipped into the subphase. The equipment used was a homemade circular Langmuir balance controlled by an electronic unit (Monofilmetter). All experiments were performed at $23 \pm 2\,^{\circ}$C.

### Penetration of AMI to phospholipid monolayers

Penetration time curves were performed by deposition of a chloroformic solution of lipids at the air/water interface, in order to form a phospholipid monolayer previous to AMI injection in the subphase. The phospholipid monolayers were initially pure DMPC or DMPC/Asc$_{16}$ (80:20). The aqueous solutions used as subphase was: Saline solution pH $\sim$5.5 (NaCl 145 mM).

### Vesicle preparation

DMPC, Asc$_{16}$, Laurdan and AMI (when accounted) were placed in appropriate amounts in glass tubes (all reagents were dissolved in chloroform-methanol, 1:1). These solutions were dried under N$_2$, to achieve a uniform film. It was kept under N$_2$ for about 1 h. Then, 300 µl of buffer (10 mM Hepes, NaCl y MgCl$_2$ a pH 7.4) were added to get a 1:2 (lipid: buffer, µg:µl) ratio. Solutions were heated by 5 min at a temperature above lipid transition and next each tube was vortexed 1 min, yielding multilamellar liposomes (MLV). To standardize the size of vesicles, the tubes were sonicated 30 min. Finally, 700 µl of buffer were added and MLV were filtered to form unilamellar liposomes with an extrusion syringe (15 times).

### DMPC + Asc$_{16}$ liposomes and DMPC + Asc$_{16}$ + AMI liposomes

Binary DMPC-Asc$_{16}$ liposomes, and ternary DMPC-Asc$_{16}$-AMI liposomes were made. The concentrations and proportions of reagents used in preparing the different liposomes are presented in Table 1. Liposomes with Laurdan were prepared to determine GP and without the probe to $\zeta$ and size particle measurements.

### Generalized polarization (GP)

Static state fluorescence spectroscopy measurements were carried out using a spectrofluorimeter SLM 4800 (SLM Instruments, Urbana, IL) and quartz cells $5 \times 5$ mm. The temperature was controlled by a circulating bath of thermostated water (Haake, Darmstadt, Germany). The temperature range was between 5 and 50 °C. The samples were excited at a $\lambda = 360$ nm, and spectra were collected in the range from 390–500 nm. From excitation spectra generalized polarization values (GP) were computed according to the following:

$$GP = (I_{434} - I_{490})/(I_{434} + I_{490}) \qquad (1)$$

where I$_{434}$ and I$_{490}$ correspond to fluorescence intensity values of the probe Laurdan to the emission wavelengths of 434 nm and 490 nm. These wavelengths are characteristic of gel and liquid-crystalline phases, respectively (Parasassi et al., 1991). Transition temperatures (T$_t$) were obtained as the zero point in the second derivative (inflection point) of the experimental GP vs. temperature curves.

### Size particle and zeta potential ($\zeta$)

The particle size, the polydispersity index (PDI) and $\zeta$ of the liposomes were determined using a Zeta sizer Nano ZS90 (Malvern Instruments, Malvern, UK). PDI is a parameter that defines the size particle distribution, more strictly, it is a dimensionless measure of the amplitude of the particle size (International Organization for Standardization [ISO] 13321, 1996). It ranges from 0–1 and is calculated according to ISO 13321 standards (ISO, 1996, Zielinska et al., 2008). PDI values between 0.1 and 0.2 indicate that the samples are monodisperse (Tantra et al., 2010).

### Stability prediction by DLVO

Virtually no heterogeneous dispersed system is completely stable. Colloidal particles system follows a continuous Brownian motion and therefore particles continuously collide with each other. In these collisions the particles can be repelled or associated in clusters and eventually attain coalescence and phase separation.

The surface charge of the particles, besides keeping them in suspension, modifies ions distribution in aqueous solution. Ions with the same charge are repelled by the surface of the particle and others with opposite charge are attracted to form a double layer.

The liposome dispersions have a high surface energy associated with the large surface area. They are thermodynamically unstable and tend naturally to cluster or merge in order to reduce its area and surface free energy.

In most of colloidal systems, liposomes in this case, the interaction forces are modeled from the DLVO theory. Details of this theory applied to liposomes are given in references

Table 1. Composition of the tested systems.

| Liposomes | DMPC (µmol) | DMPC (µg) | Asc$_{16}$ (µmol) | Asc$_{16}$ (µg) | AMI (µmol) | Laurdan (µmol) |
|---|---|---|---|---|---|---|
| DMPC (control) | 0.22 | 150 | – | – | – | – |
| DMPC + Asc$_{16}$ 10% | 0.22 | 150 | 0.022 | 9.12 | – | – |
| DMPC + Asc$_{16}$ 20% | 0.22 | 150 | 0.044 | 18.24 | – | – |
| DMPC + Asc$_{16}$ 30% | 0.22 | 150 | 0.066 | 27.36 | – | – |
| DMPC + Laurdan (0.6 µM) | 0.22 | 150 | – | – | – | $0.6 \times 10^{-3}$ |
| DMPC + Asc$_{16}$ 10% + Laurdan (0.6 µM) | 0.22 | 150 | 0.022 | 9.12 | – | $0.6 \times 10^{-3}$ |
| DMPC + Asc$_{16}$ 20% + Laurdan (0.6 µM) | 0.22 | 150 | 0.044 | 18.24 | – | $0.6 \times 10^{-3}$ |
| DMPC + Asc$_{16}$ 30% + Laurdan (0.6 µM) | 0.22 | 150 | 0.066 | 27.36 | – | $0.6 \times 10^{-3}$ |
| DMPC + Asc$_{16}$ 10% + AMI 10% | 0.22 | 150 | 0.022 | 9.12 | 0.022 | $0.6 \times 10^{-3}$ |
| DMPC + Asc$_{16}$ 10% + AMI 10% + Laurdan (0.6 µM) | 0.22 | 150 | 0.022 | 9.12 | 0.022 | $0.6 \times 10^{-3}$ |
| DMPC + Asc$_{16}$ 10% + AMI 20% | 0.22 | 150 | 0.022 | 9.12 | 0.044 | $0.6 \times 10^{-3}$ |
| DMPC + Asc$_{16}$ 10% + AMI 20% + Laurdan (0.6 µM) | 0.22 | 150 | 0.022 | 9.12 | 0.044 | $0.6 \times 10^{-3}$ |

AMI, Amiodarone; DMPC, Dimyristoylphosphatidylcholine; Asc$_{16}$, ascorbyl palmitate.

(Derjaguin & Landau, 1941; Verwey & Overbeek, 1948) and the Supplementary Material, available online.

### Stability measurements

In this section, $\zeta$ and size particle were measured as detailed in the point 2.2.5 during 28 days to carry out the stability of liposomes of: DMPC, DMPC + Asc$_{16}$ 10%, DMPC + Asc$_{16}$ 10% + AMI 10%, and DMPC Asc$_{16}$ 10% + AMI 20%. The samples were kept at 4 °C between measurements. All the measures were performed in triplicate. The stability of the liposomes of DMPC and DMPC + Asc$_{16}$ 10% was evaluated as a control.

## Results and discussion

### Adsorption on and penetration of AMI into phospholipid interfaces

We studied AMI adsorption to bare air/water interface to determinate its surface properties. When a concentrated solution of a moderately soluble amphiphile is dissolved in the bulk of an aqueous solution, the adsorption of these amphiphilic molecules to the air/water interface results in a

Gibbs monolayer, evidenced by a decrease of surface tension (increase of surface pressure) and changes in surface potential ($\Delta V$) (Figure 2a). As opposed to Langmuir monolayers (Gaines, 1966), Gibbs monolayers reflect the equilibrium between the bulk monomeric form of the amphiphile and the organized film at the interface. Figure 2(a) shows that AMI auto-organizes forming a Gibbs monolayer when diluted in the aqueous subphase, reaching surface pressure values of $34 \pm 2$ mN/m above a subphase concentration of 15 µM (see insert in Figure 2a). For a regular amphiphile the adsorption kinetic curve can be described by a hyperbolic function (Maget-Dana, 1999; Vollhardt & Fainerman, 2010; Yaminsky et al., 1996). In this case, we observed a moderate overpressure phase and a slow recovery to equilibrium values (Figure 2a). The auto-organization of the cationic amphiphile at the interface should result in a positively charged surface and the establishment of a double layer of ions, which repeals protons increasing the surface pH. Therefore, partial neutralization of the AMI molecules at the interface may occur (pKa 6.6) explaining the moderate dropping in the surface pressure values observed. A similar effect was previously described for Asc$_{16}$ adsorption to air/water interface (Mottola et al., 2013). The increase in surface



Figure 2. Surface pressure-time of Gibbs monolayers and penetration of AMI to phospholipid or phospholipid/Asc$_{16}$ monolayers. (a) Gibbs monolayer of AMI formed by adsorption to a bare air/saline solution surface and (b) penetration of AMI to DMPC monolayer (full lines) or DMPC/Asc$_{16}$ (80:20) (dashed lines) at ~30–32 mN/m. The black and gray lines and symbols in (a) and (b) correspond to surface pressure and surface potential time curves, respectively, after injection of AMI in the subphase. Final AMI subphase concentration 15.5 µM. The inset in (a), shows the final surface pressure and potential dependence with the subphase AMI concentration. The inset in (b) shows cut-off curves of AMI penetration to DMPC (black dots and black line) or DMPC/Asc$_{16}$ (80:20) (grey dots and grey line). The arrow in (b) indicates the time of AMI injection in the subphase. The curves shown are chosen from a set of duplicates that differ in less than 2 mN/m.
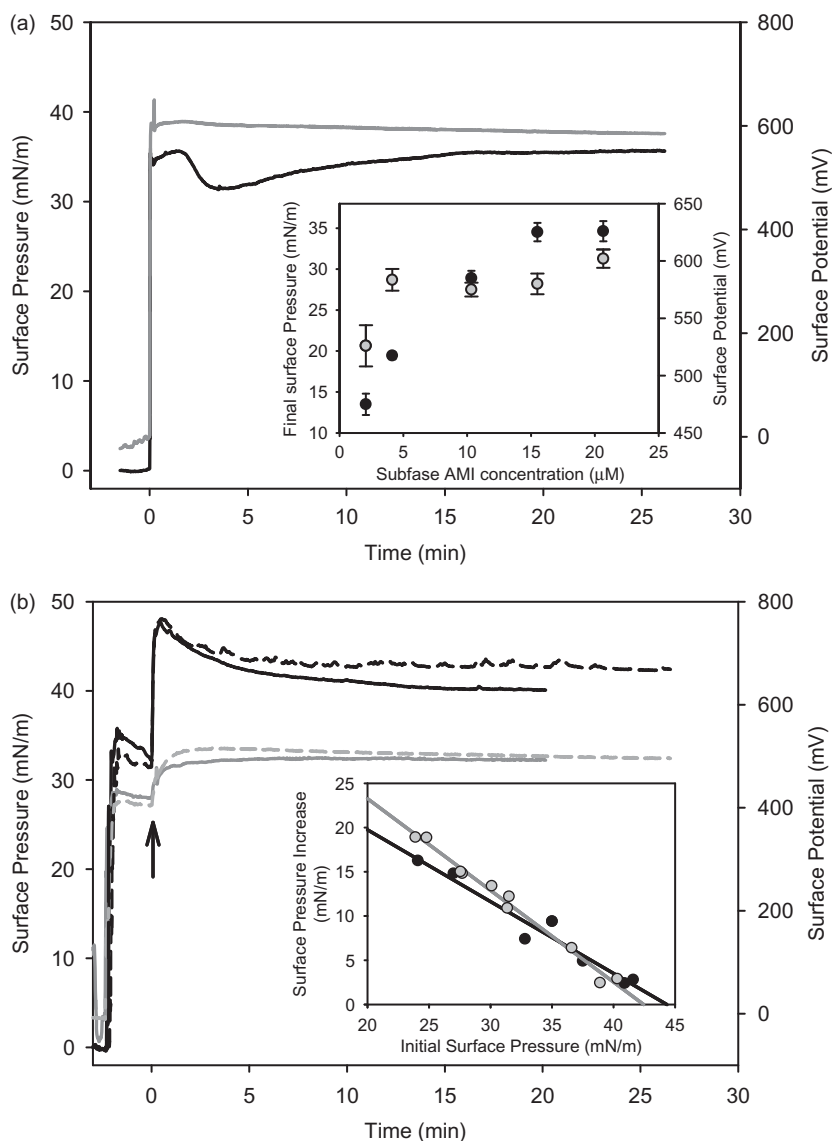
potential was also registered as a function of time showing a fast increase and stabilization to high positive values ($600 \pm 20$ mV, Figure 2a see also inset). This high value (much higher than the $50 \pm 15$ mV measured for $Asc_{16}$ monolayers and also than the $400 \pm 20$ mV observed for DMPC monolayers [Mottola et al., 2013]) may reflect the positive charged nature of the film besides other properties (the dipole moment of the AMI molecules, the induced dipole orientation of water molecules at the sub-interface and the double layer potential (Benedini et al., 2011a; Maget-Dana, 1999).

In order to explore the interaction of AMI with biomembranes, we performed studies of penetration of AMI to phospholipid monolayers. The zwitterionic lipid dimiristoyl-phosphatidylcholine (DMPC) organized in Langmuir monolayer was used as biomembrane model. At the experimental temperature DMPC monolayers have the ability to organize in a liquid-expanded phase at all surface pressures until collapse (Antunes-Madeira et al., 1995). AMI showed a good ability to penetrate DMPC monolayers (Figure 2b). It induced an increase in surface pressure reaching values of $42 \pm 2$ mN/m (when initial DMPC pressure is $30 \pm 2$ mN/m). This implies an interaction pressure of $8 \pm 2$ mN/m. The surface potential registries of the penetration experiments showed a moderate increase with AMI insertion, reaching $500 \pm 20$ mV.

To assess the possibility of using binary DMPC/$Asc_{16}$ liposomes as drug carriers, we further extended our studies to the penetration of AMI into DMPC/$Asc_{16}$ mixed monolayers. Former studies showed that the introduction of 20 mol% of $Asc_{16}$ to DMPC monolayers induces a phase transition (from liquid-expanded to liquid-condensed) at $\sim$35 mN/m with the occurrence of condensed domains in the micrometer scale that corresponds to a low area fraction ($\leq$20%). However, the transition does not lead to a complete condensed film and the two phases merges at $\sim$45 mN/m to a new phase with intermediate (expanded) properties (Mottola et al., 2013). From an examination of Figure 2(b) we can conclude that the

presence of 20 mol% $Asc_{16}$ into the DMPC monolayer slightly affect AMI penetration, showing an interaction pressure of $9 \pm 2$ mN/m (at an initial surface pressure of 30 mN/m). However, when we analyzed the increase in surface pressure ($\Delta\pi$) induced by AMI penetration at different initial surface pressures (see inset Figure 2b) we found a favorable insertion to DMPC/$Asc_{16}$ monolayers at low surface molecular packing. This difference was enhanced when we analyzed the intercept to the $\Delta\pi$ axis. This parameter is called $\Delta\pi_0$ and gave values of 36 mN/m ($r^2 = 0.95$) for pure DMPC monolayers and 44 mN/m ($r^2 = 0.99$) when containing 20 mol % of $Asc_{16}$. This difference may reflect favorable electrostatic interaction between the anionic $Asc_{16}$ and the cationic AMI amphiphiles. On the other hand, both monolayers showed similar exclusion pressures (43–45 mN/m). This implies that AMI can penetrate phospholipid membranes to surface pressures above the pressures expected for lipid bilayers ($\sim$30 mN/m).

## Biophysical state of membranes of DMPC liposomes containing $Asc_{16}$ by generalized polarization

The amphiphilic fluorescent probe (Laurdan) adsorbs to the polar region of a lipid interface and shows its solvatochromic properties (Parasassi et al., 1991). The generalized polarization (GP) is a parameter that accounts for the change in its spectroscopic properties. This value is dependent on the amount of water in the membrane, which in turn is directly related to the polarity of the surface, and indirectly to the order thereof. The structural disturbance of the bilayer of pure DMPC in presence of $Asc_{16}$ was determined by calculating GP of the Laurdan probe at different temperatures and is plotted in Figure 3(a).

The curves in Figure 3(a) showed a drop of GP when the sample is heated above $\sim$20 °C indicating the beginning of a phase transition for pure DMPC liposomes. The introduction of a second component would reduce GP values if altering the gel structure of DMPC and/or increase them when affecting
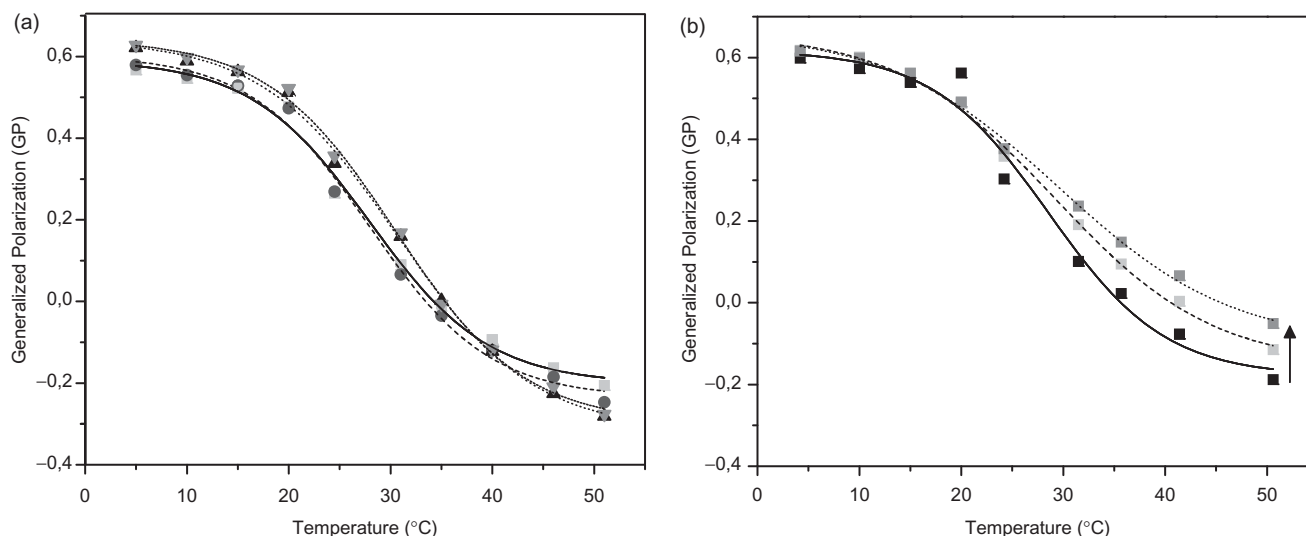
Figure 3. Changes of the generalized polarization (GP) parameter of the fluorescent probe of Laurdan depending on temperature of unilamellar liposomes from: (a) Pure DMPC (■), DMPC + $Asc_{16}$ 10% (●), DMPC + $Asc_{16}$ 20% (▲) and DMPC + $Asc_{16}$ 30% (▼). (b) Pure DMPC (■), DMPC + $Asc_{16}$ 10% + AMI 10% (■) and DMPC + $Asc_{16}$ 10% + AMI 20% (■). The arrow indicates the increase of the membrane structuration by addition of increasing amounts of AMI.

Table 2. Transition temperatures ($T_t$) vs. generalized polarization (GP) of liposomes.

| DMPC liposomes | $T_t$ (°C) |
| --- | --- |
| Control | $25.1 \pm 0.8$ |
| +$Asc_{16}$ 10% | $26.1 \pm 1.7$ |
| +$Asc_{16}$ 20% | $27.4 \pm 1.9$ |
| +$Asc_{16}$ 30% | $25.9 \pm 1.3$ |
| +$Asc_{16}$ 10% + AMI 10% | $27.1 \pm 1.1$ |
| +$Asc_{16}$ 10% + AMI 20% | $24.7 \pm 2$ |

AMI, Amiodarone; DMPC, Dimyristoylphosphatidylcholine; $Asc_{16}$, ascorbyl palmitate.

Table 3. Zeta potential ($\zeta$) and particle size of the tested systems are shown. All results were taken at day ''0''. The experiments were performed in triplicate at 28 °C.

| DMPC liposomes | $\zeta$ (mV) | Average particle size (nm) | PDI |
| --- | --- | --- | --- |
| Control | $-5.94 \pm 0.1$ | $178 \pm 3$ | $0.1 \pm 0.02$ |
| +$Asc_{16}$ 10% | $-10.6 \pm 0.2$ | $195 \pm 4$ | $0.12 \pm 0.05$ |
| +$Asc_{16}$ 20% | $-14.8 \pm 0.3$ | $159.1 \pm 15$ | $0.1 \pm 0.02$ |
| +$Asc_{16}$ 30% | $-16.5 \pm 0.5$ | $182.5 \pm 39$ | $0.13 \pm 0.03$ |
| +$Asc_{16}$ 10% + AMI 10% | $-8.35 \pm 0.1$ | $185.6 \pm 7$ | $0.1 \pm 0.06$ |
| +$Asc_{16}$ 10% + AMI 20% | $-5.33 \pm 0.2$ | $191.3 \pm 8$ | $0.18 \pm 0.05$ |

PDI, polydispersity index; AMI, Amiodarone; DMPC, Dimyristoylphosphatidylcholine; $Asc_{16}$, ascorbyl palmitate.

the liquid-crystaline phase. As it can be deduced from Figure 3(a), the presence of $Asc_{16}$ did not affect significantly the GP curve and therefore, it did not disturb the DMPC gel or liquid-crystalline phases. From the inflection point in the GP vs. temperature curves, the transition temperature ($T_t$) was obtained for both pure DMPC and with increasing concentrations of $Asc_{16}$. These values are reported in Table 2.

The $T_t$ calculated for liposomes formed by DMPC and the three different ratios of $Asc_{16}$ (10, 20 and 30%) did not differ from the $T_t$ value of pure DMPC lipid bilayer that was used as control.

### Biophysical state of membranes of DMPC liposomes containing $Asc_{16}$ and AMI by generalized polarization

Figure 3(b) shows GP vs. T curves for DMPC with $Asc_{16}$ and AMI systems in the two tested proportions. A separation of the curves from the phase transition zone was observed, which becomes more evident towards the disordered phase (indicated by an arrow in Figure 3b). However, there were not significant shifts of the phase transition temperature in respect to those of pure DMPC ($T_t \sim 23$ °C) (see Table 2). This separation of the curves towards higher GP indicates a non-homogeneous, uncooperative system and that the presence of AMI caused a small ''structuring effect'' on the disordered phase. Similar effect was reported in reference (Antunes-Madeira et al., 1995), where DMPC liposomes containing AMI were studied and its effect was evaluated by fluorescence polarization. Both in reference (Antunes-Madeira et al., 1995) and in this work, an increase in the content of AMI in the liposome affects only the fluid phase of the bilayer but not the gel phase. This result may indicate that AMI is insoluble in the gel phase and segregates in small islands but dissolves in the fluid phase thus disturbing its structure. It is worth noting that the presence of $Asc_{16}$ results in a similar effect that was reported for binary phospholipids + AMI liposomes. This indicates that this antioxidant does not generate a significant perturbation of the membrane structure of the liposome.

### Zeta potential ($\zeta$) and particle size measurements for DMPC liposomes containing $Asc_{16}$ or $Asc_{16}$ and AMI

We further characterized some physical properties of binary and ternary liposomes. Table 3 shows $\zeta$ and the average size (diameter) of particles with their respective standard deviations. In all cases we found a single peak in the particle size distribution (monomodal distribution) indicating a structural stability of the bilayer membranes. Liposomes fusion and/or fission would be evidenced by a polidisperse population. $\zeta$ reflects the net charge of the liposome plus its hydration shield and its behavior when exposed to an electric field. In most electrolyte solutions, as it is the case in our control liposomes, the $\zeta$ values for phosphatidylcholine (PC) becomes negative because of the adsorption of anions located among the zwitterionic dipoles of the polar head groups. The reported values for $\zeta$ of pure DMPC liposomes in solution span the $-5$ to $-25$ mV range (Alonso et al., 1995), depending on the ionic strength of the medium, in agreement with our findings.

Increasing the $Asc_{16}$ content in liposomes did not cause a significant change in their size and conducted to more negative $\zeta$ values. The results shown in Table 3 provide a direct evidence of $Asc_{16}$ incorporation to the membranes, since under the experimental pH ($\sim$6) $Asc_{16}$ is negatively charged. This result agrees with the monolayer experiments that show a favorable integration of $Asc_{16}$ to phospholipid membranes as said above. At low concentrations $Asc_{16}$ samples develops lamellar structures, either gel or liquid crystal. Consequently, its packing parameter is also close to unity (Palma et al., 2002), and it was expected that its inclusion in the liposomes did not alter the basic structure. On the other hand, the provision of a phospholipid environment to the $Asc_{16}$ molecules allows maintaining the flexibility properties of the liquid-crystalline liposomes, a desirable property for drug carrier function.

Table 3 also shows $\zeta$ and size of the liposomes with the addition of increasing amounts of AMI. It should be noted that $\zeta$ shifts to lower negative values with increased proportions of AMI. This is because AMI is positively charged in the experimental pH ($\sim$6). Therefore, it is expected that if the AMI proportion is increased, the $\zeta$ potential must become less negative and consequently can destabilize the system. As can be seen in Table 3, the average size of the liposomes is relatively stable with less than 0.2 PDI values indicating a monodisperse population (Tantra et al., 2010).

### Stability study of liposomes by DLVO theory

As shown in the previous paragraph, the liposome charge neutralization by the addition of AMI may affect the stability of the liposome suspension by reducing electrostatic repulsion between vesicles and promoting their fusion. To analyze this possibility we used the DLVO theory for the liposomes in

RIGHTS LINK

study. Equation 6.3 in the Supplementary Material (available online) was employed to determine $V_R$ without correction for counterion hydration and the results are presented in Figure 1 in the online Supplementary Material. This Equation was used for pure DMPC systems and with addition of 10, 20 and 30% of $Asc_{16}$. The resulting $V_{DLVO}$ potential is monotonically attractive so the liposomes should be unstable to aggregation. Since this does not occur, corrections not considered in the original DLVO theory are needed.

To take hydration forces into account, a new term was included in Equation 6.3 in the online Supplementary Material, obtaining Equation (2) (Sabín et al., 2006) . For this model, it was considered that there is a layer of hydrated counterions covering the surface of liposomes, as described in (Ohshima et al., 1982):

$$V_R = -2\pi(a + \Delta)\varepsilon_0\varepsilon_r\left(\frac{4k_BT}{ze}\gamma\right)^2 e^{[-\kappa(x+2\Delta)]} \quad (2)$$

$\Delta$ being the radius of the adsorbed hydrated ions.

In the case of liposomes of phosphatidylcholine (PC), which generally have low surface charge (<50 mV), $V_{DLVO}$ takes the following form (Sabin, 2007):

$$V_{DLVO} = -2\pi(a + \Delta)\varepsilon_0\varepsilon_r\left(\frac{4k_BT}{ze}\gamma\right)^2 e^{[-k_B(x+2\Delta)]} +$$
$$\left(-\frac{Aa}{12}\right)\left[\frac{1}{(d+2x)} - \frac{2}{(d+x)}\right.$$
$$\left. -\frac{1}{d} - 2A\ln\left(\frac{d(2x+d)}{(d+x)^2}\right)\right] \quad (3)$$

The results are represented in Figure 4, where a secondary minimum is observed in liposomes containing $Asc_{16}$. This study also evidences that the higher the $Asc_{16}$ content, the more pronounced liposome stability is predicted.

There also are some considerations regarding to the Hamaker constant, $A$, used to carry out the computations. This constant describes the van de Waals interaction between
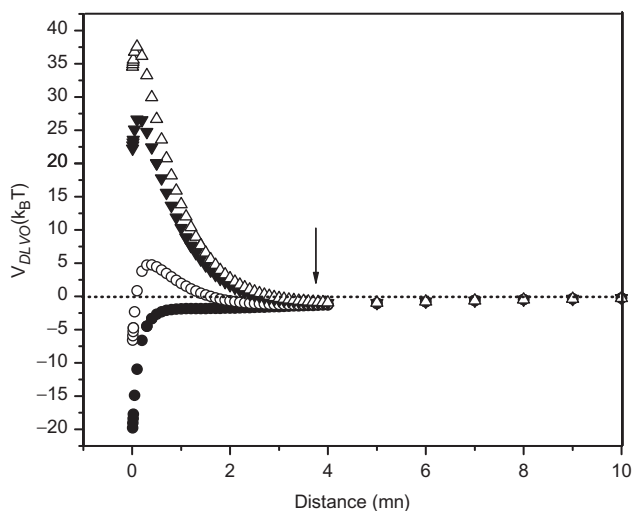
two bodies. It is in the range of $1 \times 10^{-21} - 1 \times 10^{-20}$J. In reference (Ohshima et al., 1982), in their study of the system dipalmitoyl-phosphatidylcholine (DPPC) in water Ohshima et al. (1982) estimated the Hamaker constant in $(3.6 \pm 0.8) \times 10^{-21}$J.

We took the value of this constant as that of linear hydrocarbons having 16 or more carbons, since we have worked with $Asc_{16}$ (containing a hydrocarbon chain of 16 carbon atoms) and DMPC (hydrocarbon chains of 14 carbon atoms). The Hamaker constant has two contributions as described in Equation (4).

$$A = A_{\nu=0}(2\kappa x)e^{-2\kappa x} + A_{\nu > \nu 1} \quad (4)$$

The zero frequency component of the Hamaker constant ($A_{\nu=0}$) is screened by the presence of electrolytes, while the non-zero-frequency component ($A_{\nu>0}$) is not affected by the presence of electrolytes but it is affected by the retardation effect. These components were taken as $A_{\nu=0} = -0.8 \times 10^{-21}$ J and $A_{\nu>0} \approx 6 \times 10^{-21}$ J as shown in reference (Sabin, 2007, p. 190), in the absence of electrolyte $A \approx 5.2 \times 10^{-21}$ J. This value is similar to hexadecane interacting with hexadecane through water, which was found experimentally, $A_{121} = (3-6) \times 10^{-21}$ J and reported in the literature (Israelachvili, 1991, pp. 196–197).

Retardation correction for $A_{\nu>0}$ was not considered, since it becomes significant at distances of about 5 nm or more and can be reduced to half when distance is 10 nm (Sabin, 2007, pp. 260–287), as shown in Supplementary Figure 2, available online, where $A$ is plotted as a function of the distance between the particles. As shown in Figure 4, $V_{DLVO}$ increased as we approach 1 nm, and a minimum appears at distances less than 4 nm. Therefore no correction for retardation was taken.

To compare the dependence of $A$ with distance ($x$), it was assumed that between 5 and 10 nm, $A$ decays linearly from $6 \times 10^{-21}$ J to $3 \times 10^{-21}$. It should be noted that the decay of $A$ actually has a more complex function with the distance than assumed here and there are ways to calculate it numerically solving the Lifshitz's equation (Israelachvili, 1991, pp. 196–197). However, the influence of this reduction did not affect the overall results.

The effect of changes in concentration of additives on $V_{DLVO}$ curves may be seen in Figure 4. The onset of the potential barrier is at a very short distance from the liposome surface ($\times \leq 4$ nm); at this point retardation effects are not important, and then further refinement was not considered necessary.

It can be seen that the addition of $Asc_{16}$ increases negatively $\zeta$ and the stability of the vesicles, because of the incorporation of the negatively charged $Asc_{16}$. This charge is neutralized by the addition of AMI. In Figure 5, it is shown that the $V_{DLVO}$ values decrease with the increase of the AMI proportion in the liposomes. Thus, at high concentrations of AMI in the liposomes $\zeta$ shifts to zero, and even if the hydration repulsive forces are considered in the calculation $V_{DLVO}$ becomes less than $k_BT$ when AMI concentration is above 10%, and thus liposomes must become unstable and susceptible to aggregation.

It has been determined the value of $\zeta$ ($-8.29$ mV) in which the maximum value of the potential barrier of the liposomes is



Figure 4. DMPC liposomes with $Asc_{16}$. DLVO potential ($V_{DLVO}$) vs. distance with considering the counterions' hydration. Liposome compositions were as follows: DMPC + $Asc_{16}$ 30% ($\triangle$), DMPC + $Asc_{16}$ 20% ($\blacktriangledown$), DMPC + $Asc_{16}$ 10% ($\circ$), and pure DMPC ($\bullet$). The arrow indicates the secondary minimum.

$1k_BT$, and therefore below this value the system could aggregate. This is shown in Supplementary Figure 3, available online. The proportion of AMI which gives this result in liposomes having 10% $Asc_{16}$ is 12.7%. This is shown in Supplementary Figure 4 (available online).

Since the studied liposomes were stable in all cases (even containing 20% AMI) at time 0, besides DLVO forces, there must be an additional process of stabilization, which is given by the hydrophilic character of the surface of vesicles. These repulsive hydration forces (Israelachvili, 1991, pp. 196–197) can be much stronger than the DLVO potential barrier, especially at very short distance between the approaching surfaces (distances less than 5–10 molecular diameters of the solvent, about 1–2 nm in water). These forces arise from the need to dehydrate the surfaces when the particles are close enough as to fall in the primary minimum. Since this process is energetically very costly, the system remains stable.
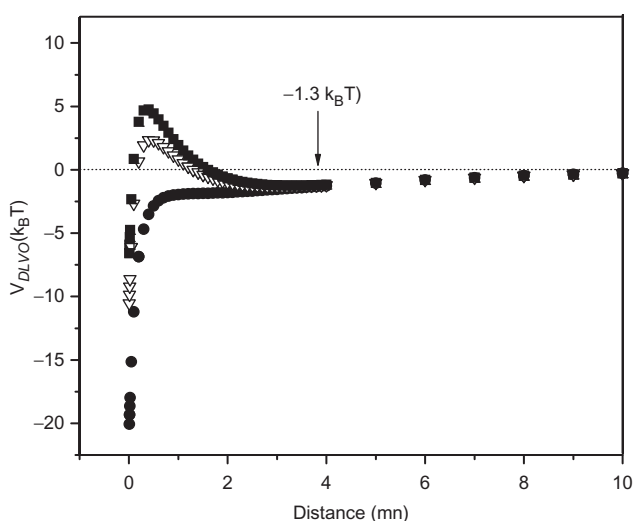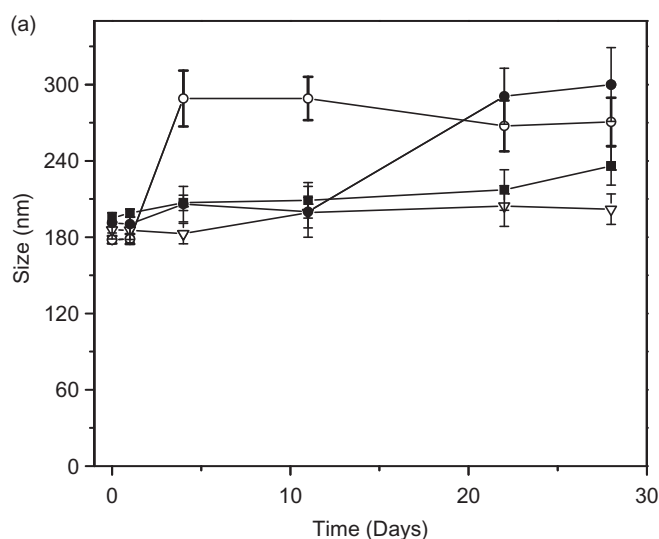


Figure 5. DLVO potential ($V_{DLVO}$) vs. distance between the particles. (■): DMPC + $Asc_{16}$ 10%, (▽) DMPC + $Asc_{16}$ 10% + AMI 10% and (●) DMPC + $Asc_{16}$ 10% + AMI 20%. The arrow indicates the secondary minimum.

## Experimental stability study of liposomes

To consider the possibility that liposomes doped with AMI could be applied in drug delivery systems, we studied their stability by measurement of the size particle (nm) and zeta potential ($\zeta$) (mV), as a function of time (days). Figure 6(a) shows that pure DMPC liposomes modified their size in the first 5 days and kept the reached size thereafter. Liposome formed by DMPC + $Asc_{16}$ kept their size stability until day 11 and then the size increase was less than 18% of the original size. DMPC + $Asc_{16}$ 10% + AMI 10% showed a stable size during all of experimental time. Finally, for DMPC + $Asc_{16}$ 10% + AMI 20% liposomes, the size particle was stable until day 11, and then started to increase up to 50% more than the original size ($\sim$200 nm). These results agree with the prediction made by DLVO modified theory. Related with the zeta potential analysis, the chart plotted in Figure 6(b) shows that the values of this parameter did not vary a large amount during the experimental time for all the samples. It is important to remark that DMPC + $Asc_{16}$ 10% + AMI 20% liposomes modified their size particle and $\zeta$ around the day 11, shifting this last parameter to more positive values. This result agrees with the previous results presented in the section entitled *Stability study of liposomes by DLVO theory*, because these liposomes were stable at time 0 but not during all the time of the experiments. Furthermore, using DLVO theory for liposomes of DMPC and 10% of $Asc_{16}$, the addition of 12.7% of AMI is enough to reach $1k_BT$, which represent the limit of AMI amount allowed in these liposomes. The liposomes with 20% of AMI were stabilized initially by other forces, as hydration forces, that likely are more important at the beginning of the experiments than DLVO repulsive and attractive forces. However, these initial stabilization forces are not energetically favorable and then, as time passed, an increment in liposome size resulted.

## Conclusion

Binary liposomes composed by phospholipid and $Asc_{16}$ behaves as a system suitable for drug delivery function. From monolayer experiments we conclude that AMI shows a
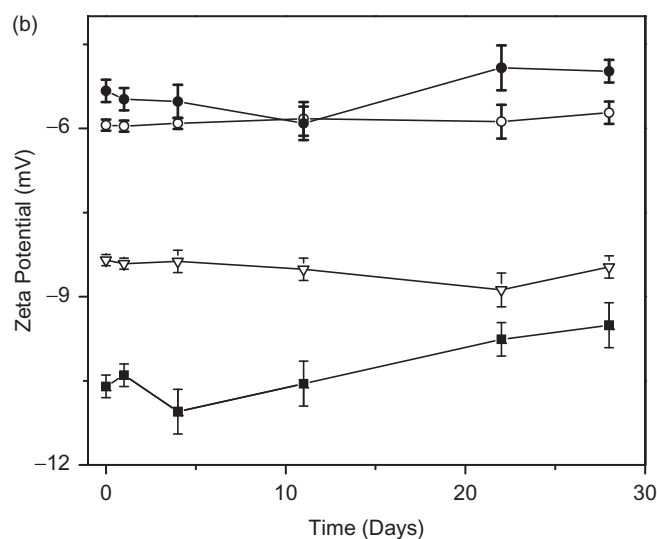


Figure 6. Liposomes stability as a function of time (days) by means of (a) size particle (nm) and (b) zeta potential ($\zeta$) (mV) Liposome compositions were as follows: (○) DMPC, (■) DMPC + $Asc_{16}$ 10%, (▽) DMPC + $Asc_{16}$ 10% + 10% AMI, and (●) DMPC + $Asc_{16}$ 10% + AMI 20%.

good surface activity (adsorption to bare air/water surface reaching equilibrium surface pressures of $\sim34$ mN/m). AMI showed a moderate but favorable propensity to penetrate phospholipid monolayers (interaction pressure 8 mN/m) that is slightly improved by the presence of 20 mol% $Asc_{16}$. The incorporation of $Asc_{16}$ molecules to liposomes and the establishment of a negatively charged surface were confirmed by ζ measurement of binary liposomes, which evidenced an increase of a negative potential with $Asc_{16}$. Furthermore, the size of the binary liposomes showed monomodal distribution that suggests stability of the system. Liposome experiments support that AMI can be incorporated to these antioxidant liposomes when they are present in a liquid-disordered state: For all tested systems ($DMPC + Asc_{16}$, with and without AMI) GP values at temperatures below $T_t$ were very similar in all studied conditions. However, above $T_t$, liposomes with AMI showed an increase in GP values depending on its concentration, indicating a structuring effect in the liquid crystalline phase of the system. Initially, the addition of AMI to liposomes formed by DMPC and $Asc_{16}$ did not change the size and stability of the liposomes. However, the incorporation of the cationic AMI molecules neutralizes the negative surface charge of the binary $DMPC + Asc_{16}$ liposomes. Due to the low electrostatic repulsion between vesicles, liposomes stability could be affected; but this has been justified by the application of the DLVO theory modified by hydration and correction of the Hamaker constant. Nevertheless, $DMPC + Asc_{16}$ 10% + AMI 10% liposomes were stable during 28 days, not only at time 0, keeping their size and zeta potential without important changes. In summary, the results shown in this work support the application of the ternary liposomes composed of phospholipids + $Asc_{16}$ + AMI as a drug delivery system. As far as we know, such a system, not previously reported in literature, appears attractive for use as a base in carrier systems for drugs that require an antioxidant activity to avoid or minimize AMI adverse effects. This is a first step in the development of these systems. A deeper study might be needed in order to focus future works to reach *in vivo* studies.

## Declaration of interest

## References

Agoston M, Örsi F, Fehér E, Hagymási K, Orosz Z, Blázovics A, et al. 2003. Silymarin and vitamin E reduce amiodarone-induced lysosomal phospholipidosis in rats. Toxicology 190:231–241.

Alonso J, Llácer C, Vila A, Figueruelo J, Molina F. 1995. Effect of the osmotic conditions on the value of 5 potential of DMPC multilamellar liposomes. Colloids Surf A: Physicochem Eng Asp 95:11–14.

Anderson N, Borlak J. 2006. Drug-induced phospholipidosis. Lipidome Dis 580:5533–5540.

Antunes-Madeira M, Videira R, Klüppelb M, Madeira V. 1995. Amiodarone effects on membrane organization evaluated by fluorescence polarization. Int J Cardiol 48:211–218.

Benedini L, Fanani L, Maggio B, Wilke N, Messina P, Palma S, Schulz P. 2011a. Surface phase behavior and domain topography of ascorbyl palmitate monolayers. Langmuir 27:10914–10919.

Benedini L, Messina PV, Manzo R, Allemandi D, Palma S, Schulz E, Frechero M, Schulz P. 2010. Colloidal properties of amiodarone in water at low concentration. J Colloid Interface Sci 342:407–414.

Benedini L, Schulz E, Messina P, Palma S, Allemandi D, Schulz P. 2011b. The ascorbyl palmitate-water system: phase diagram and state of water. Colloids Surf A: Physicochem Eng Asp 375:178–185.

Boury F, Gautier J, Bouligand Y, Proust J. 2001. Interfacial properties of amiodarone: the stabilizing effect of phosphate anions. Colloids Surf B: Biointerfaces 20:219–227.

Derjaguin B, Landau L. 1941. Theory of the stability of strongly charged lyophobic sols and of the adhesion of strongly charged particles in solutions of electrolytes. Physicochim Acta 14:633–662.

Gaines G. 1966. Insoluble monolayers at liquid-gas interfaces. New York: Interscience Publishers.

Gough W, Zeiler R, Barreca P, El-Sherif N. 1982. Hypotensive action of commercial intravenous amiodarone and polysorbate 80 in dogs. J Cardiovas Pharmacol 4:375–380.

International Organization for Standardization (ISO) 13321. 1996. Particle size analysis. Part 8: Photon correlation spectroscopy.

Israelachvili J. 1991. Intermolecular and surface forces. 2nd ed. San Diego (CA): Academic Press.

Kachel L, Moyer T, Martin W. 1990. Amiodarone-induced injury of human pulmonary artery endothelial cells: Protection by a-tocopherol. J Pharmacol Exp Therap 254:1107–1112.

Lasic D. 1998. Novel applications of liposomes. Trends Biotechnol 16: 307–321.

Lo Nostro P. 1997. Supramolecular aggregates from vitamin C derivatives: Structure and properties. Internet J Sci – Biol Chem [Online] Available at: http://www.netsci-journal.com/97v4/index.htm.

Lo Nostro P, Ninham B, Fratoni L, Palma S, Manzo R, Allemandi D, Baglioni P. 2003. Effects of water structure on the formation of coagels from ascorbyl-alkanoates. Langmuir 19:3222–3228.

Maget-Dana R. 1999. The monolayer technique: A potent tool for studying the interfacial properties of antimicrobial and membrane-lytic peptides and their interactions with lipid membranes. Biochem Biophys Acta 1462:109–140.

Mottola M, Wilke N, Benedini L, Oliveira R, Fanani L. 2013. Ascorbyl palmitate interaction with phospholipid monolayers: electrostatic and rheological preponderancy. BBA Biomembranes 1828: 2496–2505.

Ohshima H, Inoko Y, Mitsu T. 1982. Hamaker constant and binding constants of $Ca^{2+}$ and $Mg^{2+}$ in dipalmitoyl phosphatidylcholine/water system. J Colloid Interface Sci 86:57–72.

Palma S, Manzo R, Allemandi D, Fratoni L, Lo Nostro P. 2002. Coagels from ascorbic acid derivatives. Langmuir 18:9219–9224.

Parasassi T, De Stasio G, Ravagnan G, Rusch R, Gratton E. 1991. Quantitation of lipid phases in phospholipid vesicles by the generalized polarization of Laurdan fluorescence. Biophys J 60:179–189.

Ray S, Wong DV, Bagchi D. 2000. In vivo protection of DNA damage associated apoptotic and necrotic cell deaths during acetaminophen-induced nephrotoxicity, amiodarone-induced lung toxicity and doxorubicin-induced cardiotoxicity by a novel IH636 grape seed proanthocyanidin extract. Res Comm Mol Pathol Pharmacol 107: 137–166.

Sabin J, Prieto G, Ruso J, Hidalgo-Álvarez R, Sarmiento F. 2006. Size and stability of liposomes: a possible role of hydration and osmotic forces. Eur Phys JE 20:401–408.

Sabin J. 2007. Estabilidad Coloidal de Nanoestructuras Liposómicas. PhD Thesis. Santiago de Compostela, España: University of Santiago de Compostela, 93.

Stratton S, Liebler D. 1997. Determination of singlet oxygen-specific versus radical-mediated lipid peroxidation in photosensitized oxidation of lipid bilayers: effect of beta-carotene and alpha-tocopherol. Biochemistry 36:12911–12920.

Sweetman S. 2009. Martindale. The complete drug reference. 36th ed. London: The Pharmaceutical Press.

Tantra R, Schulze P, Quincey P. 2010. Effect of nanoparticle concentration on zeta-potential measurement results and reproducibility. Particuology 8:279–285.

Vereckei A, Blazovics A, György I, Fehér E, Tóth M, Szénási G, et al. 1993. The role of free radicals in the pathogenesis of amiodarone toxicity. Cardiovasc Electrophysiol 4:161–177.

Verwey E, Overbeek J. 1948. Theory of stability of lyophobic colloids. Amsterdam, Netherlands: Elsevier.

Vollhardt D, Fainerman V. 2010. Characterization of phase transition in adsorbed monolayers at the air/water interface. Adv Colloid Interface Sci 154:1–19.

Yaminsky V, Ninham B, Stewart A. 1996. Surface activity and ion exchange, a study via surface tension, wetting tension and surface force techniques. Langmuir 12:836–850.

Yasaka W, Eichbaum F, Oga S. 1979. Antiarrhythmic effects of solvents: III. Effects of propylene glycol and benzyl alcohol on contractile force of isolated rabbit heart. Cardiovasc Res 13: 717–722.

Zielinska K, Wilk K, Jezierski A, Jesionowski T. 2008. Microstructure and structural transition in microemulsions stabilized by aldonamide-type surfactants. J Colloid Interface Sci 321: 408–417.